NUMERICAL STRUCTURAL ANALYSIS OF NPP REINFORCED CONCRETE STRUCTURES UNDER SEISMIC LOADING

NUMERYCZNA ANALIZA STRUKTURALNA ŻELBETOWYCH KONSTRUKCJI ELEKTROWNI JĄDROWYCH W WARUNKACH OBCIĄŻEŃ SEJSMICZNYCH

Vladimir Aleshin, Vadim Seleznev

Physical & Technical Center, LLC, Russian Federation
vva@ptc.sar.ru, sve@ptc.sar.ru

Abstract:The paper describes an approach to the numerical analysis of response of nuclear power plant buildings including soil-structure interaction effects. A reinforced concrete structure of an NPP reactor building under operating and seismic loadings is considered. The simulated seismic load corresponds to a maximum designed earthquake of magnitude 7 (the peak ground surface acceleration is 0.12 g). The numerical analysis was performed by the finite element method in a 3D nonlinear statement using the FEM-programs ANSYS and LS-DYNA. Review of the numerical analysis results demonstrated that the presented technique can be successfully applied to seismic design of NPP structures.

Keywords: nuclear power plants, seismic loading, reinforced concrete structures, multiaxial stress state, numerical structural analysis, finite elements.

Streszczenie: W artykule opisano sposób analizy numerycznej reakcji (odpowiedzi) budynków elektrowni jądrowej, łącznie ze zjawiskami interakcji pomiędzy gruntem a konstrukcjami. Rozpatrywana jest żelbetowa konstrukcja budynku reaktora elektrowni jądrowej w warunkach roboczych i obciążeń sejsmicznych. Symulowane obciążenie sejsmiczne odpowiada maksymalnej sile trzęsienia ziemi założonej w projekcie, a mianowicie poziomowi 7 (maksymalne szczytowe wartości przyspieszenia gruntu wynoszą 0,12g). Analiza numeryczna została wykonana przy użyciu metody elementów skończonych dla trójwymiarowego modelu nieliniowego z wykorzystaniem programów ANSYS oraz LS-DYNA służących do analizy MES. Przegląd wyników analiz numerycznych wykazał, że zaprezentowana technika może być z powodzeniem stosowania do projektowania konstrukcji elektrowni jądrowych z uwzględnieniem zagrożeń sejsmicznych.

Słowa kluczowe: elektrownie jądrowe, obciążenie sejsmiczne, konstrukcje żelbetowe, stan naprężeń wieloosiowych, numeryczna analiza strukturalna, elementy skończone

1. Introduction

Earthquakes belong to the most dangerous acts of nature for structures, buildings and equipment of nuclear power plants (NPP). Therefore, national and international safety standards provide requirements for seismic design of each NPP [1–10]. For example, in accordance with Ref. [1], seismic response of structures should be provided at horizontal ground surface accelerations of at least 0.1 *g* for each newly designed NPP, irrespective of exposure to seismic risks in the region, where it will be constructed. IAEA regulations contain the same requirement to NPPs under design [9, 10].

The disaster at the Fukushima-I and Fukushima-II NPPs in Japan in spring 2011 demonstrated that traditional methods of computational seismic analysis of critical NPP structures require improvement, especially with respect to strong earthquakes. When developing computational methods for seismic analysis of structures, consideration should also be given to the fact that seismic waves act together with operating loads. For example, mechanical load on a reactor building (which is the most critical NPP structure) that should be incorporated in numerical analysis of seismic effects includes internal pressure; dead weight of structures and equipment; nonlinear structure-soil interaction (SSI). For prestressed containment structures, one should also add load from tension of tendons. Thus, NPP structures are always combined loaded under earthquakes.

2. Problem statement

In the general case, mathematical modeling of seismic response of NPP reinforced concrete structures is a classical dynamic problem of solid mechanics [11, 12]. Problem statement for the propagation of seismic waves in the soil does not reach beyond the widely known mathematical models and methods of solid mechanics. Applied methods for computational analysis of structure seismic response that are currently used and are being actively developed can globally be classified in three ways: model dimensionality (spring-damper-mass systems, 1D, 2D, 3D); material models for structure and soil (linear or nonlinear, isotropic or anisotropic, uniform or nonuniform etc.); SSI models (fixed base, kinematic coupling, force coupling, contact pair etc.). Depending on the problem statement, seismic response of a structure can be simulated in different ways: from analytical solutions (for the simplest cases) to various versions of grid methods.

In rectangular Cartesian coordinate system $(x_1; x_2; x_3)$ multiaxial stress states of a solid structure and soil base under dynamic loading on the assumption of infinite small strains are described by the following set of equations [11]:

$$\sigma_{ij,j} - \rho a_i + \rho b_i = 0; \tag{1}$$

$$\varepsilon_{ij} = 0.5\left(u_{i,j} + u_{j,i}\right); \tag{2}$$

$$\varepsilon_{ki,jl} + \varepsilon_{lj,ik} - \varepsilon_{li,jk} - \varepsilon_{kj,il} = 0, \tag{3}$$

for the defined boundary conditions

$$u_i = u_i^*(t), \ x \in \Gamma_1; \tag{4}$$

$$\sigma_{ij} n_j = p_i(t), \ x \in \Gamma_2; \tag{5}$$

$$\left(\sigma_{ij}^+ - \sigma_{ij}^-\right) n_j = 0, \ x \in \Gamma_3, \tag{6}$$

and initial conditions

$$u_i = u_i^0; \ \dot{u}_i = \dot{u}_i^0; \ t = 0; \ x \in V, \tag{7}$$

where σ_{ij} are components of the Cauchy stress tensor; ρ is the material density; a_i are components of the acceleration vector; b_i are components of the body force vector; ε_{ij} are components of the strain tensor; u_i are components of the displacement vector; "$,j$" is the operator of partial differentiation with respect to the spatial coordinate "$\partial/\partial x_j$", $i, \ j, \ k, \ l = 1, 2, 3$; t is the time; $u_i^*(t)$ is the time law for the components of the displacement vector at the points on the boundary surface Γ_1; $p_i(t)$ is the time law for the components of the surface force vector at the points on the boundary surface Γ_2; $\sigma_{ij}^+, \sigma_{ij}^-$ are components of the stress tensor to the right and to the left of the discontinuity surface (contact) Γ_3, respectively; $\Gamma_1 \cup \Gamma_2 \cup \Gamma_3 \subset \Gamma$; Γ is the boundary surface of the structure; n_i are components of the unit outward normal to the boundary surface; dotted variable is the operator of time differentiation ($\dot{u}_i = \partial u_i/\partial t$); V is the structure volume; x is a point in the 3D space. In (1) and below in the paper, it's assumed that corresponding terms of equations are summed up by repeated subscripts.

In order to complete the system (1–7), one should add physical equations, the form of which is determined by the involved mathematical models that build upon experimental research into macroscopic physical and mechanical properties of materials. In particular, for all the materials used in reinforced concrete structures, just as for NPP site soils, corresponding physical equations can be represented in the general form as smooth or piecewise smooth functions dependent on the stress tensor, strain (strain rate) tensor, and other physical parameters, which determine the multiaxial nonlinear stress state of a structure (soil) in each particular case of solid mechanics problem definition [12]:

$$f\left(\sigma_{ij}, \ \varepsilon_{ij}, \ \dot{\varepsilon}_{ij}, T, t, \chi_i\right) = 0, \tag{8}$$

where $\dot{\varepsilon}_{ij}$ are components of the strain rate tensor; T is the temperature; χ_i are additional material parameters (for example, governing material hardening/softening laws). In addition to the physical nonlinearity of materials properties, modeling of the multiaxial stress state of NPP reinforced concrete structures under strong earthquake conditions may also require incorporating the geometric nonlinearity of deformations. For this purpose, the linear Cauchy relations (2) obtained on the assumption of infinitely small strain should be replaced by nonlinear Green equations containing second-order summands [11]:

$$\varepsilon_{ij} = 0.5\left(u_{i,j} + u_{j,i} + u_{k,i} u_{k,j}\right). \tag{9}$$

The relations (1) and (3) in Cartesian coordinates will transform accordingly [12]. The explicit form of Eq. (8) is determined based on the choice of the material's mathematical model. In response to mechanical load, all grades of reinforced concrete [13–16] and all types of mineral soils [17–19] display linear elastic properties at the initial stage of deformation. The linear elastic behavior of materials is most commonly described by Hooke's Law:

$$\sigma_{ij} = E_{ijkl}\varepsilon_{kl}, \tag{10}$$

where E_{ijkl} are components of the elasticity tensor. As it is known, because of the symmetry of the elasticity tensor in the pairs of subscripts (i,j) and (k,l), only 36 of its 81 components are independent. The elasticity tensor with 36 independent components describes the behavior of a linearly elastic anisotropic material. If the material possesses any geometric symmetry of its properties, the number of independent components E_{ijkl} decreases. For example, all components of the elasticity tensor for an orthotropic material are defined by nine independent material parameters, and for an isotropic material, by two [12]. All grades of concretes [14] and steels for reinforcement [20] used for NPP construction have isotropic physical and mechanical properties in fairly good approximation. Prestress tendons are braided of wire made from high-strength grades of steel and, consequently, its material also possesses isotropic physical properties (on a single-wire scale).

Thus, in order to model the initial state of NPP structures and buildings and to analyze their multiaxial stress state under seismic load, one should have credible values of two independent parameters of elastic materials. The most convenient parameters include standard engineering characteristics: Young's modulus E and Poisson ratio ν (or shear modulus G). These characteristics are known to be related to each other as $G = 0.5E(1+\nu)^{-1}$.

In order to allow for thermal strain resulting from variations in the material temperature, the expression (1) should be replaced by the known Duhamel-Neumann equation obtained based on the additivity of elastic and thermal strain established experimentally:

$$\sigma_{ij} = E_{ijkl}\left(\varepsilon_{kl} - \alpha_{kl}\Delta T\right), \tag{11}$$

where α_{kl} is the tensor of thermal expansion coefficients; ΔT is the temperature difference. A uniform material has a diagonal tensor of thermal expansion coefficients, i.e. $\alpha_{kl} \neq 0$ only if $k = l$. For a uniform isotropic material, the expression (11) is additionally simplified, because the tensor α_{kl} becomes spherical $\alpha_{kk} = \alpha, (k = 1, 2, 3)$.

Reinforced concrete is a heterogeneous composite material, which possesses anisotropy (basically, orthotropy) in all physical and mechanical properties, except thermal expansion coefficients, depending on the type and direction of reinforcement. In order to save computational resources, the composite material of

reinforced concrete structures can be idealized as a uniform anisotropic (in the general case) material with effective linear elastic properties. Corresponding algorithms and mathematical models are described in detail in [19].

The most reasonable way to solve the set of equations (1–7) as applied to the analysis of the multiaxial stress state of reinforced structures and soil is the direct displacement method [11]. As basic unknowns, this method uses displacements of structure points defined as functions of spatial coordinates in chosen coordinate system of the 3D Euclidean space. Then, using the geometric relations (2) and physical equations (8), one can express stresses in terms of displacements and insert the resulting expressions into (1). If the displacement method is used, the strain compatibility equations (3) are satisfied automatically and are not used in the problem solution.

With the linear elastic isotropic material model and on the assumption that deformations are infinitely small, application of the displacement method to the solid dynamics problem leads to the known Lame equations [11]:

$$(\lambda + \mu)\,\theta_{,i} + \mu\,\Delta u_i - \rho\,\ddot{u}_i = 0, \tag{12}$$

where λ, μ are the Lame parameters; $\theta = \varepsilon_{ii}$ is bulk strain; Δ is the Laplace operator. The Lame parameters can be expressed in terms of engineering characteristics of elastic properties of the material $\lambda = 2\nu G/(1-2\nu)$, $\mu = G$;

The initial conditions (7) for NPP buildings and structures are defined based on the results of solving a separate boundary-value solid mechanics problem in the static statement [11]. Such a problem statement is sufficient for adequate modeling of operating and additional failure static and quasi-static loads included in the seismic analysis (dead weight, prestress, internal pressure etc.). The static problem statement can be obtained, if in (1) $\rho a_i = 0$ is taken in accordance with d'Alembert's principle [12]. In this case, the boundary conditions (4–6) are time-independent, and no initial conditions (7) are required. As applied to static problems, the Lame equations are elliptic [19]. It is reasonable to use finite elements method (FEM) [21] as the most efficient method of numerical analysis of NPP reinforced concrete structures.

3. On the modeling of soils at NPP sites

Let us discuss the formulation of models providing credible description of the multiaxial stress state of soils at NPP sites under operating and seismic loads. The formulation of the models described below is based on the approaches, mathematical models and soil modeling methods discussed in [19]. Most of mineral soils are treated within solid mechanics as granular-like, loosely coupled geomaterial without noticeable hardening under moderate mechanical load. This circumstance allows us to model soils as an elastic-perfectly plastic material with pressure-dependent yield. As a condition for the transition to the plastic state, soil mechanics uses Mohr's envelope [19]:

$$|\tau_n| = \Phi(\sigma_n),\tag{13}$$

where τ_n and σ_n are the tangent and normal stress components on a surface element with the normal $\vec{\mathbf{n}}$; $\Phi(\sigma_n)$ is a non-decreasing function. In the general case, $\Phi(\sigma_n)$ is nonlinear. For cohesionless soils and cohesive soils under moderate pressure $\Phi(\sigma_n)$ can be represented as a linear Coulomb equation [18]:

$$|\tau_n| = c + \tan\varphi \cdot \sigma_n,\tag{14}$$

where c is specific cohesion; φ is the angle of internal friction of the soil. The parameters c and φ characterize physical properties of the soil and are determined experimentally. It follows from physical considerations that the values of these parameters are non-negative.

In soil mechanics, compressive stress is traditionally assumed positive (14). Turning to the more convenient treatment of compressive stress as negative and extending the Coulomb criterion (14) to the three-dimensional stress state, the following yield condition is obtained:

$$|\sigma_1 - \sigma_2| = (2c \cdot \cot\varphi - \sigma_1 - \sigma_2)\sin\varphi; \quad |\sigma_2 - \sigma_3| = (2c \cdot \cot\varphi - \sigma_2 - \sigma_3)\sin\varphi;$$
$$|\sigma_3 - \sigma_1| = (2c \cdot \cot\varphi - \sigma_3 - \sigma_1)\sin\varphi,\tag{15}$$

where $\sigma_1, \sigma_2, \sigma_3$ are principal values of the stress tensor. When plotted in the principal stress space, the condition (15) can be represented as a hexahedral pyramid called the Mohr-Coulomb pyramid, the axis of which is equally inclined to the axes of principal stresses and, consequently, coincides with the hydrostatic axis $\sigma_1 = \sigma_2 = \sigma_3$. The apex of the Mohr-Coulomb pyramid has coordinates $\sigma_1^* = \sigma_2^* = \sigma_3^* = c \cdot \cot\varphi$.

The criterion (14) possesses certain drawbacks, which become rather significant, when it comes to numerical modeling (19). Without going into details, it should be noted here that within the generally used approach to three-dimensional soil mechanics simulations the piecewise-linear Mohr-Coulomb surface is approximated by a smooth yield surface of the form:

$$f(I_1, J_2, J_3) = 0,\tag{16}$$

where $I_1 = \sigma_{ii}$ is the first invariant of the stress tensor; $J_2 = s_{ij}s_{ij}/2$ is the second invariant of the stress tensor; $J_3 = s_{ij}s_{jk}s_{ki}/3$ is the third invariant of the stress tensor; s_{ij} are components of the stress tensor deviator, $s_{ij} = \sigma_{ij} - I_1/3$. By applying convolution of the tensor product, invariant parameters of the complex stress state in (16) can be expressed in terms of the principal values of the stress tensor in the following way:

$$I_1 = \sigma_1 + \sigma_2 + \sigma_3; \quad J_2 = \frac{1}{6}\left[(\sigma_1 - \sigma_2)^2 + (\sigma_1 - \sigma_2)^2 + (\sigma_1 - \sigma_2)^2\right];\tag{17}$$

$$J_3 = \frac{1}{27}\left[2(\sigma_1^3 + \sigma_2^3 + \sigma_3^3) - 3(\sigma_1^2\sigma_2 + \sigma_2^2\sigma_3 + \sigma_3^2\sigma_1 + \sigma_1\sigma_2^2 + \sigma_2\sigma_3^2 + \sigma_3\sigma_1^2) + 12\sigma_1\sigma_2\sigma_3\right]. \quad (18)$$

Writing the criterion (16) in terms of invariant parameters (17) and (18) may lead to cumbersome expressions. Therefore, for compact expression of some mathematical models one often uses another set of invariants of complex stress state [22]:

$$p = -\left(\sigma_1 + \sigma_2 + \sigma_3\right)/3; \qquad q = \sqrt{1.5 s_{ij}s_{ij}}; \qquad r = \left(4.5 s_{ij}s_{jk}s_{ki}\right)^{1/3}. \quad (19)$$

As it is seen from (19), p is hydrostatic pressure, and q is equivalent (von Mises) stress. The invariant parameters (17), (18) and (19) are related with each other as follows: $p = -I_1/3$; $q = \sqrt{3J_2}$; $r = 3\left(0.5J_3\right)^{1/3}$. Mathematical representation of limit surface equations for soils can be further simplified by introducing an additional parameter of multiaxial stress state θ, a polar angle in the deviator plane (the Lode angle) [19]:

$$\cos\left(3\theta\right) = 3\sqrt{3}J_3\big/\left(2J_2^{3/2}\right) \text{ or } \cos\left(3\theta\right) = \left(r/q\right)^3. \quad (20)$$

In practice, the forms of smooth approximation for the Mohr-Coulomb surface that are used most often include various modifications of the extended Drucker-Prager criterion [19, 22]:

$$t^* - p \cdot \tan\beta' - d = 0, \quad (21)$$

where $t^* = 0.5q\left[1 + K^{-1} - \left(1 - K^{-1}\right)\cos\left(3\theta\right)\right]$; β', d, K are constitutive parameters determined directly by stabilometry of soil samples [17] or calculated in accordance with standard physical and mechanical properties of soils. Examination of (21) using the mathematical apparatus of analytical and differential geometries shows [19] that the criterion (21) in the principal stress space is visualized by a surface of a linear nonround cone. The principal axis (axis of symmetry) of cone coincides with the hydrostatic axis, just as with the Mohr-Coulomb pyramid.

It seems the most reasonable to approximate Mohr-Coulomb criterion (14) using the Menétrey-Willam yield surface [23]. Applying the expressions for invariant parameters of multiaxial stress state (19) and the Lode angle (20), the Menétrey-Willam yield criterion for soils can be written as:

$$\sqrt{\left(\varepsilon c \cdot tg\varphi\right)^2 + \left[R_{mw}\left(\theta\right)q\right]^2} - p \cdot \tan\varphi - c = 0, \quad (22)$$

where ε is the meridional eccentricity, that defines the rate at which the hyperbolic line in the meridional plane approaches the linear asymptote;

$$R_{mw}\left(\theta\right) = \frac{4\left(1 - e^2\right)\cos^2\theta + \left(2e - 1\right)^2}{2\left(1 - e^2\right)\cos\theta + \left(2e - 1\right)\sqrt{4\left(1 - e^2\right)\cos^2\theta + 5e^2 - 4e}} \frac{3 - \sin\varphi}{6\cos\varphi};$$

e is the deviatoric eccentricity, that describes the "out-of-roundedness" of the deviatoric section. In practical implementation of the criterion (21), one should

take into account that the function $R_{mw}(\theta)$ is discontinuous in the domain of the argument $0 \le \theta \le 2\pi$. Therefore, Eq. (22) can be used to construct only a sixth of the Menétrey-William yield surface for $0 \le \theta \le \pi/3$. In the segment $[0; \pi/3]$ the function $R_{mw}(\theta)$ belongs to the class $C^{(1)}$. Considering symmetry, the remaining parts of the surface can be easily recovered by geometric transformations of the initial expression, including rotations along the hydrostatic axis and reflections with respect to the corresponding meridional planes in the principal stress space. The Menétrey-Willam yield surface (22) will be a smooth approximation of the Mohr-Coulomb criterion (15) for soils assuming that $e = K$, where $K = (3 - \sin\varphi)/(3 + \sin\varphi)$ [19].

4. On the modeling of seismic effects

Now, let us consider the sources of seismic waves, or earthquake origins [24–26]. Geomechanically, earthquakes are strong dynamic effects of tectonic nature. Tectonic stresses accumulating in the earthquake origin and acting in its small area – focus or hypocenter – produce a rupture in the material of the earth's crust (shock). Energy released with the fast stress relief is dispersed in the form of elastic stress waves traveling from the shock focus in all directions at velocities from several hundred to several thousand meters per second. Fig. 1 shows a schematic representation of an earth shock. The projection of the hypocenter onto the earth's surface is called epicenter.

The strength of earth shocks at any location on the earth's surface depends primarily on the distance from the earthquake focus to the given point, and structure of the earth's crust along the path of seismic waves. For quantitative assessment of the earthquake strength, one uses two basic characteristics – shock intensity or magnitude. The first characteristic represents the scale of damage caused by an earthquake, and the second is a measure of seismic energy released with an earth shock. The maximum number of levels, or classes, on currently used earthquake intensity scales is twelve. There are several measurement scales, but in Russia only one of them is used, namely the 12-degree Medvedev-Sponheuer-Karnik scale (MSK-64), which is also internationally used. This scale provides for the following levels of earthquake intensity: 1–3, weak; 4–5, perceptible; 6–7, strong; 8, damaging; 9, destructive; 10, devastating; 11, catastrophic; 12, very catastrophic.

The Richter magnitude is defined as a logarithm of the ratio of the amplitude of seismic waves A to the amplitude of some reference earthquake A_s: $M = \log(A/A_s)$.

There also exist other ways to calculate the magnitude. Earthquake intensity in the epicenter and magnitude are related fairly conventionally: $I_0 = 1.7M - 2.2$; or, considering the depth of the earthquake focus H: $I_0 = \tilde{a}M - \tilde{b}\log H + \tilde{c}$, where $\tilde{a}, \tilde{b}, \tilde{c}$ are coefficients determined empirically for a specific seismic region. Attenuation of seismic waves is also estimated empirically and is visualized by isolines called isoseists on seismic maps. As shown in Fig. 1, in the epicenter, the earth's surface vibrates mostly vertically, while the role of the horizontal component increases with distance from the epicenter.
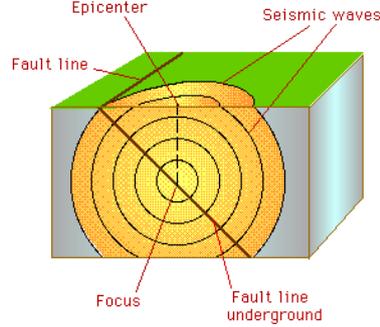
Fig. 1 Schematic representation of an earthquake origin.

The only more or less useful quantitative characteristic for deterministic numerical modeling could be the so-called earthquake energy $\tilde{E} = \pi^2 \rho \tilde{V} \left(a_A / \tilde{T} \right)$, where ρ is the density of the earth's upper layers; $\tilde{V}$ is the velocity of waves; a_A is the amplitude of displacement; and $\tilde{T}$ is the period. If it is assumed that the values of all these characteristics are proved, then the Lame equation (12) can be solved analytically by the method of characteristics for the case of plane waves [11]. The plane wave describes the motion of unchanged configuration in the direction of a unit vector $\bar{\mathbf{n}}$ at a velocity $\tilde{c}$. One can demonstrate that strict solutions of this type, corresponding to the constant configuration-independent velocity $\tilde{c}$ are possible only in unbounded linear elastic continuum [11]. The field of displacements corresponding to the plane wave is given by the following expressions:

$$\tilde{u}_i = U_i \left(\tilde{c} t - n_s x_s \right). \tag{23}$$

Inserting (23) into (12) gives a set of homogeneous linear equations, which has a nontrivial solution if its determinant is zero:

$$\det \left\| (\lambda + \mu) n_i n_s + \mu \delta_{is} - \rho \tilde{c}^2 \delta_{is} \right\| = 0. \tag{24}$$

For isotropic materials, wave velocities are equal in all directions, so in (24) one can take $n_1 = 1$, $n_2 = n_3 = 0$. If we insert these values into (24), calculate the determinant and solve the resulting equation, we will see that it has one unrepeated and one repeated root. Consequently, in isotropic unbounded linear elastic continuum, there are only two velocities of plane waves that are found from the solution of (24):

$$\tilde{c}_1 = \sqrt{(\lambda + \mu) / \rho}; \quad \tilde{c}_2 = \sqrt{\mu / \rho}, \tag{25}$$

where $\tilde{c}_1$ is the velocity of longitudinal (compressional) waves; $\tilde{c}_2$ is the velocity of transverse (shear) waves. Note that in the absence of more specific data, velocities of longitudinal and transverse waves of real earthquakes are estimated using the formulas (25), derived for a much more idealized case than the structure of the earth's crust. Using the model of isotropic linear elastic medium, one can also show that waves propagating in bounded domains (like half-space) as a result of stress relief on the boundary surface produce two types of surface waves, whose intensity decays with depth [11] – the Love and the Rayleigh waves. These types of waves are also observed during earthquakes and belong to secondary seismic

waves, but they have much lower velocities and energies in comparison with compressional and shear waves. Therefore, the surface waves have a small effect on structural damage caused by earthquakes.

Thus, numerical modeling of seismic waves is done only for the assessment of their global propagation all over the earth. Application of this approach to the analysis of seismic effects on specific buildings and structures is unreasonable because most of basic data are lacking and it is hard to provide detailed (on the structure scale) numerical simulations of waves in a heterogeneous body of soil extending to hundreds and thousands of kilometers even with supercomputers.

For simulation of the structure seismic response, it is sufficient to represent seismic waves traveling through the area, where it is located, as broadband random ground motion in three dimensions [27]. In turn, complex modes of three-dimensional seismic soil vibrations can be conventionally reduced to simultaneous but statistically independent horizontal and vertical components. Kinematic characteristics (acceleration, velocity, displacement) of such components are determined experimentally based on seismographic records representing components of corresponding characteristics of the soil surface as a function of time in the chosen Cartesian coordinate system [24]. Earthquake records generally include accelerograms, which are time histories of acceleration components. Time histories of velocity and displacement components on the soil surface can be obtained by integration of available accelerograms.

The strong motion portion of severe earthquakes may be from 10 to 15 seconds, although the total duration of shocks is considerably longer [27]. Thus, it is sufficient to perform numerical transient structural analysis of the structure under intensive seismic load over a period of no more than 20 seconds.

Another peculiarity of seismic load is that the maximum amplitude of horizontal components of the soil surface motion is overwhelmingly (unless the affected structure is situated in the epicenter) higher than the maximum amplitude of the corresponding vertical component [26, 27]. This circumstance is due to the difference in the total energy release in the earthquake origin conveyed by the compressional and shear seismic waves. As shown by the relations (25), longitudinal waves have the maximum velocity and, accordingly, the highest energy. They are the first to reach the site, where structures are located. Therefore, the maximum damage to buildings and structures caused by earthquakes results from compressional waves in soil. In this connection, special attention in seismic recording is paid to accelerograms of horizontal ground surface motion components. In the absence of specific data on the maximum acceleration of vertical soil motion near the site, one can assume that the ratio of maximum values of vertical and horizontal accelerations varies in the range of 1/2 to 1 [10]. The specific value depends on many factors, such as the distance from the earthquake hypocenter, soil properties etc. In practical simulations, this ratio is generally assumed to be 2/3 [10, 25, 27].

5. Methods of seismic analysis of NPP structures

As noted above, in order to obtain high accurate results, the numerical analysis of multiaxial stress state of NPP structures should be done with three-dimensional FE

models. National and international regulations [3–10] offer three basic methods for seismic analysis of NPP structures, buildings and equipment: equivalent static, response spectrum, and transient dynamic analysis. These methods differ in the application of seismic load, for example, to buildings on foundations and equipment located in the buildings. The scope of this paper is limited to the methods for modeling the load on buildings. It is also supposed that as input seismic data accelerograms on the free-field soil surface are used.

Equivalent static analysis is the most straightforward and computationally least expensive method. In this analysis an equivalent static load is applied to the sole (foundation) of a structure. The equivalent static load is corresponded to the absolute maximum on accelerogram. Inertial and dissipative properties of real materials and structures are taken into consideration using linear coefficients (dynamic amplification factors). The method was widely used in the past, under the conditions of considerable shortage of computational resources. At present, application of this method is limited to simple structures with strongly marked predominance of one mode shape, for example, high cantilever-type structures. On the other hand, due to the development of commercial FE-programs, the method continues to be employed, because it readily allows for nearly any physical nonlinearity or nonuniformity of structures. Note that this method produces the most conservative estimates.

Response spectrum analysis can be done comparatively quickly on commodity computers. As applied to dynamic solid mechanics equations, the method uses expansion of mass, stiffness and damping matrices in mode shapes of a structure. This makes application of this method to the analysis of any structures, other than linear uniform, unreasonable and basically inappropriate. An additional drawback of the method is that it gives only response amplitudes for each mode shape. As the solution contains no data on response phases, in order to reduce superfluous conservatism, one should use special methods for summing up the different modes: Square Root Sum of Squares (SRSS); Complete Quadratic Combination (CQC); Absolute Sum (ABS) etc. [27].

Transient dynamic analysis is the most credible method that can produce results of practically useful accuracy allowing for physically and geometrically nonlinear behavior of all structures. As this method is computationally expensive, its application has been limited until recently. At present, transient nonlinear dynamic analysis of NPP structures, such as reactor containment, can be done on commodity computers. Therefore, this method gains ground in seismic analysis of NPP buildings and structures under design.

Another important issue for the technology of numerical analysis of NPP structures is SSI modeling. The simplest case is NPP location in stiff grounds belonging to seismic category I. In this case, international and national regulations allow direct application of seismic load to the foundation, which significantly simplifies the problem to be solved. However, category I grounds are virtually rocky, and it is quite uncommon to choose them for NPP construction. Numerical analysis of seismic effects should include stiffness and dissipation properties of soils belonging to category II and III. At present, there are several ways of such modeling.

The only way of SSI modeling available in the past and widely used at present is simplified representation by mass-spring-damper systems. Formulas for calculating equivalent masses, damping and stiffness coefficients of these systems are available in Standard [3].

As of today, however, the most credible way of seismic analysis of NPP buildings is 3D modeling of contact between structure and soil base. The size of the FE model of the soil base should be large enough to preclude unphysical structure response to seismic waves reflected from the boundary. As preliminary estimates show, should boundary conditions of the soil base be like those that are generally used for solid finite elements, the size of the FE model of such a soil body will be too large for running such simulations on commodity computers. This situation can be resolved to some extent by defining lumped-damper boundary conditions that can absorb waves running from the structure. This method is called convolution of boundary conditions [27]. In this method, however, in addition to the excessive complexity of model development, damping coefficients are unknown in advance and need to be fitted iteratively. In addition, even after the fitting of acceptable values, all the waves caused by an earthquake cannot be absorbed completely.

A better solution to the problem is to define soil boundaries as special rows of three-dimensional finite elements that absorb the energy of seismic waves. Recent releases of advanced FEM programs offer such features, although they are still in the beta releases [28, 29].

6. Examples of application

In accordance with the problem statement described in Sect. 2 and based on the mathematical models and methods presented in Sects. 3–5, a technology for numerical analysis of multiaxial nonlinear stress state of NPP reinforced concrete structures under operating and failure loads, including earthquakes, was developed. As numerical modeling tools for the technology development FEM programs ANSYS Release 14.0 and LS-DYNA 971 R5.1.1 were used [28, 29]. The computational model of the inner containment of the reactor building at the Baltic NPP is shown in Fig. 2.

The structure of the inner containment was modeled together with the anchorage gallery and mat foundation. Other structures of the reactor building and associated equipment were not considered at this stage and not included in modeling. Soil was simulated as a laminated structure with horizontal layers. Each layer possessed its own physical properties given in Table 1. The model included only the soil layer below the sole of the mat foundation. This is because the reactor building is surrounded by other buildings of the NPP nuclear island nearly all the way along its perimeter. Each of these buildings has its own foundation, and they are separated only by narrow aseismic gaps. The computational model of the soil base contained additional layers of special solid FEs to absorb seismic waves.

Modeling of the multiaxial stress state of the containment structure is done by successive application of loads in accordance with actual conditions of the NPP reactor building: dead load; tension of tendons; internal pressure and temperature; seismic excitation.

Seismic load on the containment model was defined by time histories of parameters of a real earthquake [24–27]. As prescribed by the regulations, the maximum amplitudes of these time histories were scaled to the required level of a maximum design earthquake of magnitude 7 (0.12g). Examples of the numerical simulation

results are shown in Figs. 3–5. In these figures, the FE mesh and some parts of the computational model are hidden for better illustration.
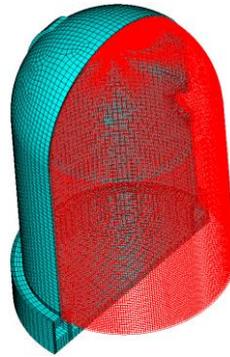

Fig. 2. Computational model of the reinforced concrete structure of the NPP inner containment.
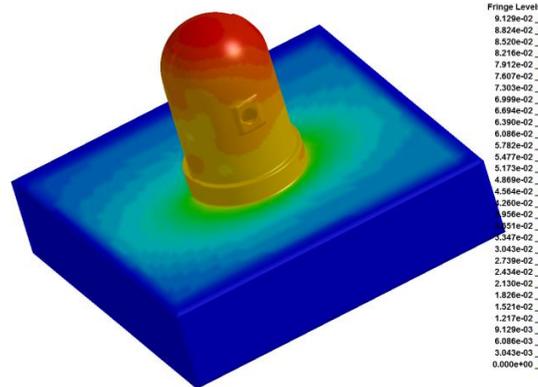

Fig.3. Velocities [m/s] in the containment structure and soil under seismic load corresponding to a maximum design earthquake of magnitude 7
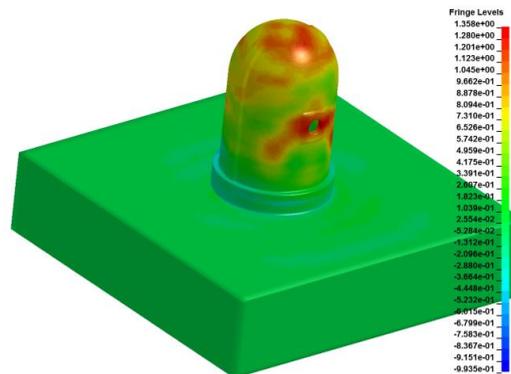

Fig. 4. Accelerations[m / s^2] in the containment structure and soil under seismic load corresponding to a maximum design earthquake of magnitude 7
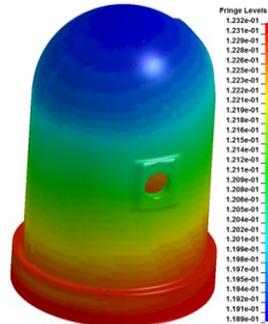
Fig. 5. Displacements [m] in the containment structure under seismic load corresponding to a maximum design earthquake of magnitude 7

Table 1. Standard physical properties of soils at NPP site

Type of soil	Characteristics			
	Density, kg/m^3	Specific cohesion, kPa	Angle of internal friction, °	Young's modulus, MPa
Glacial varves (lg III):				
- loam (IGE-6v)	1960	24	23	12
- sand (IGE-8)	2030	2	32	27
- varve clay (IGE-6a)	1860	38	14	11
Moraine (g III):				
- sandy clay (IGE-9)	2220	21	30	25
- loamy clay (IGE-10a)	2090	47	20	20
Lower Cambrian and Upper Proterozoic deposits (C_1Pt_3kt):				
- clay (IGE-14)	2140	42	18	35
- sand (IGE-13)	2020	3	37	22
- sandstone	2160	34	42	150

7. Conclusion

The paper describes an approach to numerical analysis of interaction between reinforced concrete NPP structures and soil under seismic load. As a simulation object transient seismic response of a reinforced concrete structure of an NPP reactor building to a maximum design earthquake of magnitude 7 (0.12 g) was considered. This problem was solved by the FEM in a 3D nonlinear statement using the ANSYS Release and LS-DYNA programs. Review of the numerical analysis results demonstrated that the presented technique can be successfully applied to seismic design of NPP structures.

8. References

[1] Accounting for Natural and Technology-Related Effects on Nuclear and Radiation-Dangerous Sites. PNAE G-05-035-94. Gosatomnadzor of Russia, Moscow, 1995 (in Russian).

[2] Design Guidelines for Aseismic Nuclear Power Plants. NP-031-01. Gosatomnadzor

of Russia, Moscow, 2001 (in Russian).

[3] Seismic Analysis of Safety-Related Nuclear Structures and Commentary. ASCE 4-98. ASCE Standards, USA, 2000.

[4] Code for Seismic Design of Buildings. National Standard of the People's Republic of China. GB 50011-2001, Beijing, 2001.

[5] British Standard Specification for Prestressed Concrete Pressure Vessels for Nuclear Engineering. BS 4975, UK, 1990.

[6] Règles de conception et de construction du génie civil des ilots nucléaires REP. Code RCC-G, éditions AFCEN, France, 2007 (in French).

[7] Technical Guidelines for Aseismic Design of Nuclear Power Plants. JEAG 4601-1991 Supplement, Japan Electric Association, 1991.

[8] Eurocode 8: Design Provisions for Earthquake Resistance of Structures. ENV 1998-1-6:2004, CEN, Bruxelles, 2004.

[9] Seismic Design and Qualification for Nuclear Power Plants. Safety Guide, Safety Standards Series No. NS-G-1.6. IAEA, Vienna, 2003.

[10] Evaluation of Seismic Hazards for Nuclear Power Plants. Safety Guide, Safety Standards Series No. NS-G-3.3. IAEA, Vienna, 2002.

[11] Rabotnov Yu.N. Solid Mechanics. Nauka, Moscow, 1988 (in Russian).

[12] Sedov L.I. Continuum Mechanics. Nauka, Moscow, 1984. V.2 (in Russian).

[13] Nonprestressed Concrete and Reinforced Concrete Structures. SP 52-101-2003. Gosstroi of Russia, Moscow, 2004 (in Russian).

[14] GOST 26633-91. Heavy and Fine Grain Concretes // Specifications. USSR Gosstroi, Moscow, 1991 (in Russian).

[15] Murray Y.D. User Manual for LS-DYNA Concrete Material Model 159. Publication No. FHWA-HRT-05-062. The Federal Highway Administration (FHWA), USA, 2007.

[16] CEB-FIP Model Code 1990. Design Code. Comité Euro-International du Béton. Thomas Telford House, London, 1993.

[17] Tsitovich N.A. Soil Mechanics. Higher School, Moscow, 1983 (in Russian).

[18] Governing Laws of Soil Mechanics // Collection of papers, Mechanics: New Developments in Foreign Science Series / Ed. A.Yu. Ishlinsky and G.G. Chernyi. Issue 2. Mir, Moscow 1975 (in Russian).

[19] Seleznev V.E., Aleshin V.V., Pryalov S.N. Mathematical Modeling of Piping and Ductwork Systems: Methods, Models and Algorithms. MAKS Press, Moscow, 2007 (in Russian).

[20] GOST 5781-82. Hot-Rolled Steel for Concrete Reinforcement. RF Goskomstandart, 1983 (in Russian).

[21] Zienkiewicz O.C., Taylor R.L. The Finite Element method. Butterworth–Heinemann, Oxford, 2000.

[22] Chen W.F., Han D.J. Plasticity for Structural Engineers. Springer–Verlag, New York, 1988.

[23] Menétrey Ph., Willam K.J. Triaxial Failure Criterion for Concrete and its Generalization // ACI Structural Journal, vol. 92, May/June, 1995.

[24] Aki K., Richards P. Quantitative Seismology, W.H. Freeman and Company, San Francisco, 1980.

[25] Nonlinear Seismic Correlation Analysis of the JNES/NUPEC Large-Scale Piping System Tests / Ali S.A, Nie J., DeGrassi G., et al. // Proceedings of 2008 ASME Pressure Vessels and Piping Division Conference, Paper PVP2008-61881, Chicago, IL, USA, 2008.

[26] Geotechnical Aspects of Site Evaluation and Foundations for Nuclear Power Plants. Safety Guide, Safety Standards Series No. NS-G-3.6. IAEA, Vienna, 2004.

[27] Cooper P., Hoby P., Prinja N. How to Do Seismic Analysis Using Finite Elements. NAFEMS Ltd., Glasgow, 2007.

[28] ANSYS Mechanical APDL Documentation. Release 14.0. SAS IP, Inc., 2011.

[29] LS-DYNA Theory Manual / Compiled by J.O. Hallquist // Livermore Software Technology Corporation, 2006.

Vadim Seleznev, Doctor of Science, Professor. *Vadim Seleznev received his PhD degree from the Russian Federal Nuclear Center – All-Russian Scientific Institute of Technical Physics in Snezhynsk and his DSc degree from Moscow Power Engineering Institute (Technical University). Vadim Seleznev has the Russian State Certificate of Professor. Prof. Seleznev has coauthored 9 books and has over 190 publications on various aspects of computational fluid dynamics, numerical thermal analysis and mathematical optimization. He is past Deputy Chief Designer of the Russian Federal Nuclear Center – All-Russian Scientific Institute of Experimental Physics in Sarov. Currently, Prof. Seleznev is First Deputy Director of the Physical and Technical Center in Sarov, Russia.*

Vladimir Aleshin, Doctor of Science. *Vladimir Aleshin received his PhD degree from Moscow Power Engineering Institute (Technical University) and his DSc degree from Russian State Academy of Fire Service in Moscow. Dr. Aleshin has coauthored 9 books and has over 130 publications on various aspects of continuum mechanics, numerical structural and thermal analyses. He is past Deputy Chief of Division of the Russian Federal Nuclear Center – All-Russian Scientific Institute of Experimental Physics in Sarov. Currently, Dr. Aleshin is Deputy Director of the Physical and Technical Center in Sarov, Russia.*